Article

Not peer-reviewed version

Study on Fabrication and Properties of Polyvinyl Alcohol—Chitosan Nanofibers from Aqueous Solution with Acetic Acid and Ethanol by Electrospinning Method

Thi Hong Nhung Vu * , Svetlana N. Morozkina , Roman O. Olekhnovich , Aleksandr V. Podshivalov , Mayya V. Uspenskaya

Posted Date: 4 October 2024

doi: 10.20944/preprints202410.0296.v1

Keywords: poly(vinyl alcohol); chitosan; biomaterials; electrospinning; fiber technology; targeted drug delivery system

Article

Study on Fabrication and Properties of Polyvinyl Alcohol—Chitosan Nanofibers from Aqueous Solution with Acetic Acid and Ethanol by Electrospinning Method

Thi Hong Nhung Vu [1,*], Svetlana N. Morozkina [2,3], Roman O. Olekhnovich [3], Aleksandr V. Podshivalov [3] and Mayya V. Uspenskaya [4]

[1] Vietnam National University of Forestry at Dong Nai, Trang Bom District, Trang Bom Town, Dong Nai Province, Vietnam
[2] Kabardino-Balkarian State University, Chernyshevskogo 173, Nalchik, Russia
[3] Chemical Engineering Centre, ITMO University, Kronverkskiy Prospekt, 49A, 197101 St. Petersburg, Russia
[4] Peter the Great State St. Petersburg Polytechnic University, Russia
* Correspondence: vuhongnhungs@gmail.com; Tel.: +84982290029

Abstract: Drug–targeted integrated nanofiber development is a current research trend. Potential materials for the development of such systems include Poly (vinyl alcohol) (PVA) and chitosan (CS) nanofibers, which are traditionally fabricated by electrospinning aqueous solutions of these polymers with acetic acid. To improve drug integration, the binary-solvent system was converted into a multi–solvent system by the adding of ethanol. This caused noticeable shifts in the solvent system's solubility parameter, the interaction of the various component forces, and optical and rheological properties of PVA-CS solution. The results show that solution containing 4% PVA, 3% CS, 15% ethanol and 45% acetic acid is optimal for the increasing of manufacturing productivity, improving the morphology and diameter of PVA–CS nanofibers, without changing in chemical bonding composition. The XRD spectrum revealed that the alterations in the crystal lattice and diameter of the PVA–CS nanofibers leaded to the variation in their thermal and tensile properties.

Keywords: poly(vinyl alcohol); chitosan; biomaterials; electrospinning; fiber technology; targeted drug delivery system

1. Introduction

The development of targeted drug delivery systems is actual research for medicine. Nanofiber–based drug delivery system represents a system that works by the delivering of the drug to the diseased cell. This helps to reduce the dose of drugs, to avoid the wasting of drug, thereby reducing the amount of drug to be produced, and reducing the economic burden. In addition, this also allow to avoid the side effects of the drug or the tendency to become drug–resistant in patients. PVA–CS nanofibers are one of the potential targeted drug delivery systems.

Fabrication of PVA – CS nanofibers by electrospinning is very attractive research towards drug integration for drug delivery targeting purposes. PVA and CS polymers have been confirmed to be non–toxic, biosafe, biocompatible [1–8] and have a wide range of applications in the industrial, food and especially medical industries [1,6–13]. The combination of PVA and CS improves the moisture–sensitive properties of PVA and the insolubility of CS, increasing the stability of the system. In the drug delivery system, due to its hydrophilic nature, PVA helps the composite material easily cross in the body to the organs. Apart from that, because of the polysaccharide structure, being a basic and positively charged polyamine, CS is soluble only in the acidic environment of diseased cells in the

 doi:10.20944/preprints202410.0296.v1

body, CS serves as a guiding system for drug delivery and release. Basically, healthy cells have a pH between 7.1 and 7.4 [14,15], whereas most diseased cell types have an acidic environment, and depending on the cell type and the condition of the injury, their pH can drop even to 4.7 in fracture–related hematomas [14–17]. Thus, the combination of PVA and CS not only improves the properties of the polymer system, but also shows the potential for an excellent synergy of biological activities of the two materials. This type of composite material utilizes the water–soluble advantage of polyvinyl alcohol for drug delivery and the advantage of CS in the targeting of the acidic and negatively charged arears of diseased cell types. PVA–CS nanofibers are particularly suitable for the integration of drugs whose molecules are capable to form hydrogen bonds.

Usually, studies on these nanofibers were carried out with the use of acetic acid aqueous solvents [18–22]. In practice, drugs are often organic compounds that are soluble in less polar solvents, so a decrease of the polarity of the solvent system is more likely to incorporate a higher amount of the drug. Besides, the PVA – CS solution in acidic aqueous solution has quite high electrical conductivity, leading to the fabrication of nanofibers which also requires more stringent electrospinning parameters.

Ethanol is a volatile, inexpensive, readily available, essentially non–toxic solvent that can be used to dissolve a wide variety of organic compounds. The addition of ethanol to polymer solutions has great potential to improve the integration of organic compounds in general and drug integration in particular, especially ethanol–soluble compounds, into composite systems.

In an efforts to find the optimal conditions for the fabrication of drug–integrated nanofibers, we investigated the effect of ethanol in acetic acid solution system on the electrospinning of PVA–CS nanofibers. The effect of electrospinning solution contents on the chemical composition, crystal structure, and thermomechanical properties of PVA–CS nanofibers was also investigated.

2. Materials and Methods

2.1. Materials

Polyvinyl alcohol with a molecular weight 75 kDa and CS with a molecular weight of 200 kDa were purchased from LenReaktiv company, acetic acid 99.5%, ethanol 95% and distilled water were used as the solvents.

2.2. Optical Properties of Polymer Solutions

To study the optical density of polymer solutions, a UNICO 2150-UV device (USA) with a wavelength range of 200–1000 nm was used.

A turbidity meter 2100P HACH, model 2100P CAT. No 44740–88 (Germany) was used to investigate the turbidity of polymer solutions. The accuracy is ±2%, the resolution is 0.01 FNU, and the reproducibility is ±1%.

2.3. Rheological Properties

The pH of the electrospun solutions was determined using a Mettler Toledo S213 SevenCompact Duo pH/conductivity meter. pH precision is 0.002.

The dynamic viscosity of polymer solutions was determined using an MCR 502 rheometer with a cylinder. Shear rate ranging from 0.1 to 500s–1 was measured at 25°C.

The conductivity of the polymer solution was measured using the WTW inoLab Cond 7110 conductivity meter with the WTW TetraCon 325 sensor and the Mettler Toledo S213 SevenCompact Duo pH/conductivity meter (accuracy was ± 0.002 pH).

2.4. Electrospinning Technique

To investigate fiber fabrication parameters, an electrospinning system NANON–01A (MECC CO., LTD., Fukuoka, Japan) was used. The electrospinning was carried out at the temperature of 28.0 ± 2.0 °C and the relative humidity of 21 ± 3 %. The following technological specifications were investigated to facilitate the electrospinning process: voltage ranges from 16 to 30 kV; feed rate ranges

 doi:10.20944/preprints202410.0296.v1

from 0.1 to 0.4 mL/h; needle to collector distances range from 120 to 150 mm; horizontal speed 10 mm/s; 16G steel needle; 150 mm x 200 mm (L x B) stainless steel receiver plate.

The rotating drum of the device at 500 rpm was used to obtain the nanofiber matrix for mechanical properties investigations.

2.5. Morphology and Diameters of Nanofibers

The preliminary characteristics, morphologies, and diameters of PVA electrospinning fibers were determined using the Olympus STM6 (OLYMPUS Corporation, Tokyo, Japan) measuring optical microscope. The differential interference contrast (DIC) technique was used to emphasize the color and contrast of the reaped fibers. The microphotographs program ImageJ (National Institutes of Health, Bethesda, MD, USA) was used for analysis and measurement of the electrospun nanofiber diameter.

2.6. Fourier–Transform Infrared (FTIR) Spectroscopy

A Bruker alpha Fourier transform infrared spectrometer (Bruker, Germany) was used to obtain the samples' infrared absorption spectra. The investigated spectral range was between 4000 and 500 cm–1.

2.7. X–ray Diffraction (XRD) Analysis

At the room temperature, wide–angle X–Ray diffraction (XRD) profiles of polymer powders and nanofibers were obtained using a DRON–8 X–Ray unit in a slit configuration with a BSV–29 sharp confocal tube with a copper anode and a NaI (Tl) irradiation probe and a β–filter (Ni). XRD was performed on flat surface samples placed on glass slides. The 2θ range of the samples was 10–60°. The average crystallite size was calculated using the Scherrer formula:

$$\tau = K \lambda/\beta \cos \theta$$

where τ = average crystallite size, K = shape factor (0.98 rad), λ = X–ray wavelength (1.54 Å), β = the line broadening at half the maximum intensity (FWHM) and θ = Bragg angle. The normalized area of the diffraction peaks was used to calculate the degree of crystallinity [23].

2.8. Differential Scanning Calorimetry (DSC) Analysis

Differential scanning calorimetry (DSC) was performed using a DSC 204 F1 Phoenix instrument (Netzsch, Germany). The experiments were carried out in nitrogen–filled closed aluminum crucibles (protective gas flow rate of 80 mL/min, working gas flow rate of 30 mL/min). Approximately 2 mg of samples were heated and cooled at the rate of 10 K/min in a temperature range of up to 300°C. Prior to analysis, samples were heated from the room temperature to 150 °C to remove the adsorbed moisture. After 5 minutes at 150 °C, samples were cooled to –30 °C and then analyzed in the –30 °C to +300 °C temperature range. The comparison cell consists of air.

The heat scan was used to calculate the samples' degree of crystallinity (χc) using the following equation:

$$\chi c = (\Delta H/m\ \Delta H_o) \times 100$$

where m is the mass of PVA, ΔH is the melting enthalpy of the sample, and ΔH_o is the fusion enthalpy of 100% crystalline PVA, which has been reported to be 150 J/g [24].

2.9. Thermogravimetric Analysis (TGA)

The thermogravimetric properties of the initial polymers and the resulting nanofibers were investigated using a TG 209 F1 Libra vacuum–tight microthermal balance (Netzsch, Germany). The temperature range was 25°C to 900°C, the heating rate was 10°C/min, the nitrogen gas atmosphere flow rate was 40 mL/min, and the measuring cup material was Al_2O_3.

 doi:10.20944/preprints202410.0296.v1

2.10. Tensile Property

The Instron 5943 tensile testing machine was used to investigate the tensile properties of samples (Instron, USA). The test was carried out at the room temperature and at the speed of 50 mm/min in accordance with the ISO 527–3 standard [25].

2.11. Statistical Analysis

OriginPro 2019b was used to investigate the diameter distribution of materials and nanofibers from micrographs (OriginLab Corporation, Northampton, MA, USA).

To determine the lattice parameters of PVA powder, CS powder, and nanofibers, the DSC and XRD data were analyzed using OriginPro 2019b and X'Pert Highscore software (PANalytical, 2009), as well as the DICVOL04 indexing program.

3. Results and Discussion

In this study, all concentrations and ratios were calculated as mass percent % (wt/wt) concentrations and simply denoted as %.

The best mixture solution composition for the PVA-CS nanofibers fabrication from the same polymer components using a CH_3COOH-H_2O solvent system was found as 4% PVA, 3% CS, and 60% CH_3COOH in the previous publication [26]. As a result, in this investigation, the polymer and water propotions were maintained while adjusting the acetic acid/ethanol ratio to achieve a total concentration of 60%.

3.1. Effect of Ethanol– Acetic Acid Ratio on Optical Properties of PVA–CS Solution

An aqueous solutions containing 4% PVA, 3% CS, and a mixture of ethanol and acetic acid solvents in different ratios were prepared, with the total organic solvent content of 60%. The turbidity and the optical density of the resultant solutions were determined at the wavelength of 425 nm.

There are several effects that occur when the ethanol concentration in a solution is increased, and the concentration of acetic acid is decreased. These include the reducing of the acidity and polarity of the PVA-CS solution, as well as the replacing of acetic acid with ethanol in hydrogen bonding with the polymers.

The results presented in Table 1 and on Figure 1 demonstrate that although the concentration of each polymer and the concentration of water remained constant, the absorbance (A) and turbidity of the solution changed as the ethanol–acetic acid ratio were altered.

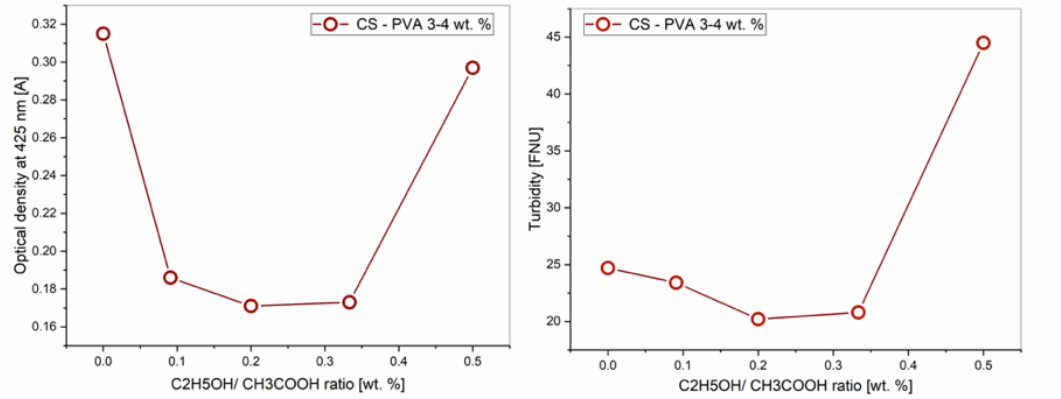

Figure 1. Effect of the ethanol–acetic acid ratio on the optical density and turbidity of the PVA–CS solution.

 doi:10.20944/preprints202410.0296.v1

Table 1. Effect of the ethanol–acetic acid ratio on the optical density and turbidity of the PVA–CS solution.

CH_3COOH/C_2H_5OH, %	Optical density		Turbidity, FNU
	Absorption (A)	Transmission (T), %	
60/0	0,315	48,4	24,7
55/5	0,186	65,2	23,4
50/10	0,171	67,4	20,2
45/15	0,173	67,2	20,8
40/20	0,297	50,5	44,5

According to the Mie theory, the absorbance (A) of a solution of identical particles at a particular wavelength (λ) of light is described by the formula:

$$A = \log_{10}\left(\frac{I}{I_0}\right)$$

Where I_0 is the incident light intensity, and I is the light intensity after the passing through the solution. By the using of the extinction cross–section σ, path length l, and number density N, the relationship between I and I_0 is given in the publication [27]:

$$I = I_0 e^{-\sigma l n}$$

The absorbance (A) can be represented by the formula:

$$A = \frac{\sigma l N}{ln10}$$

For spherical particles, the extinction cross–section (σ) is related to the extinction efficiency (Q_{ext}) by $\sigma = \pi R2Q_{ext}$, where R is the spherical particle's radius [28]

$$A = \frac{\pi R^2 Q_{ext} l N}{ln10}$$

A solution model with a particle size distribution's actual absorption spectrum is the total of the weighted sum of the absorption spectra of all the particle sizes:

$$A = \sum_{n=1}^{i} W_i A_i$$

where n is total particle sizes in the distribution, Wi and Ai are the weight and absorbance of ith particle size, respectively:

$$A = \frac{\pi N}{ln10} \sum_{n=1}^{i} R_i^2 Q_{ext,i} W_i$$

And number density N denotes the total number of particles in the solution per unit volume [29].

This means that an increase of the ethanol concentration and a decrease of the acetic acid concentration significantly affect the size of polymer nanoparticle suspensions, as well as their solubility. The replacement of acetic acid with ethanol reduced the number of hydrogen bonds in the solution and lessened the size and mass of the nanoparticles. It is the dwindling of the nanoparticle size that causes a diminution of the optical density and turbidity of the solution at ethanol concentration below 20%.

When the ethanol concentration reached 20% and the concentration of acetic acid decreased to 40%, the pH and polarity of the solution were insufficient for the complete polycation of CS formation. This leads to a decrease of the solubility of CS and the onset of phase separation. As a result, both the optical density and the turbidity of the solution sharply increased. When the ratio of ethanol–acetic acid reaches 25–35, the PVA–CS solution is no longer obtained.

A diversification in the combination state of polymers under the influence of the ethanol–acetic acid ratio significantly affects the rheological properties, especially the viscosity of PVA–CS solutions.

 doi:10.20944/preprints202410.0296.v1

3.2. Effect of Ethanol– Acetic Acid Ratio on Rheological Properties of PVA–CS Solution

The aqueous solutions containing 4% PVA, 3% CS and a mixture of ethanol and acetic acid solvents in different ^ratios such that the total concentration of the organic solvents was 60% were prepared. The rheological properties of these solutions were then investigated (Figure 2).

The flow curve of a PVA–CS 4–3 solution under the influence of different ratios of ethanol–acetic acid also shows the character of a complex flow with three stages: destruction of the initial structure of the solution when applying shear rates of less than 1.5 s^{-1}, Newtonian models of fluid flows with shear rates from 1.5 to 10 s^{-1} and non–Newtonian models with shear rates greater than 10 s^{-1}.

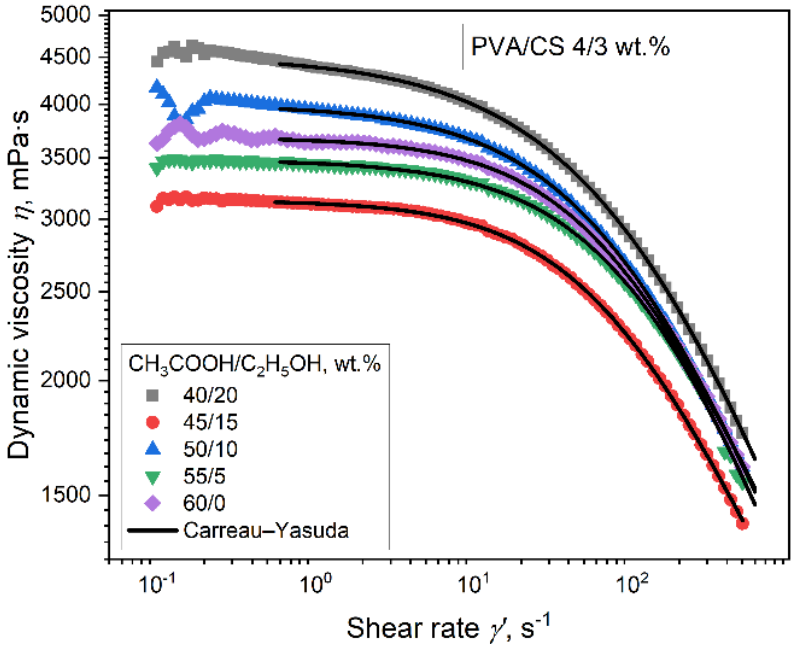

Figure 2. Graphs of the dependence of shear rate from the dynamic viscosity of PVA–CS solutions at the different ratios of ethanol–acetic acid.

The Carreau–Yasuda model of non–Newtonian liquid flow was applied for a complex description of the flow of solutions in the second and third ranges [30,31].

$$\eta(\dot{\gamma}) = \eta_0[1 + (\lambda\dot{\gamma})^a]^{\frac{m-1}{a}}$$

where η_0 is the zero shear viscosity, λ is the characteristic time constant, a is the change of flow type, and m is the flow (pseudoplasticity) index. On Figure 2, the fitting curves of the Carreau–Yasuda equation are shown as black lines. The parameters of the Carreau–Yasuda equation for the curves (Figure 2) are presented in Table 2.

The values of the coefficient of determination show that the model describes the considered shear rate ranges almost perfectly. It can be seen that the values of η0, which characterize the total viscosity of the solution in the second range of shear rates, change in a complex manner with an increase of the ethanol–acetic acid ratio.

Table 2. The parameters of the Carreau–Yasuda equation for PVA–CS solutions at the different ratios of ethanol–acetic acid.

CH_3COOH/C_2H_5OH, (%)	η_0, (mPa·s)	$\lambda \cdot 10^3$ (s)	*a*	*m*	R^2
60/0	3678	13,86	0,93	0,611	0,9999
55/5	3479	7,11	0,84	0,507	0,9995
50/10	3993	11,54	0,80	0,553	0,9999

 doi:10.20944/preprints202410.0296.v1

45/15	3143	13,70	0,92	0,617	0,9999
40/20	4511	7,56	0,68	0,485	0,9999

In this case, the flow rate m represents the dependence from the ratio of ethanol–acetic acid. The flow index m is less than 1, which characterizes the active liquefaction of the system.

The complex variation in the values of viscosity η0 and the flow index m of PVA–CS solutions under the influence of the ethanol–acetic acid ratio is associated with a modification in the structure and combinatorial state of macromolecules in the solution. Alterations in the size of nanoparticles, particle density, and polymer solubility, in addition to adaptations of the values of optical density and turbidity, obviously had a significant effect on the rheological properties of PVA–CS 4–3 solution.

The pH, viscosity and electrical conductivity of PVA–CS 4–3 solutions under the action of ethanol– acetic acid ratios are measured and presented in Table 3 and on Figure 3.

Table 3. Effect of ethanol– acetic acid ratio on rheological property values of PVA–CS solution.

C_2H_5OH/ CH_3COOH, (%)	pH	Viscosity η, (mPa·s)	Electrical conductivity 3, (μS / cm)
0/60	2.02	2724.3	1611
5/55	2.25	2644.6	1541
10/50	2.48	2796.7	1505
15/45	2.71	2338.4	1434
20/40	2.90	3036.7	1402

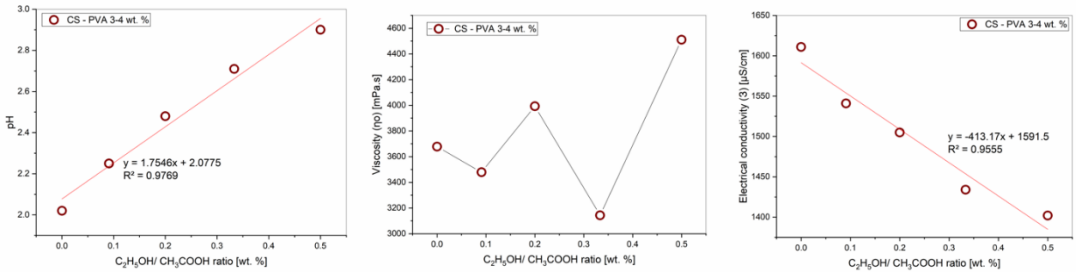

Figure 3. Graphs of the dependence of the rheological property values of the PVA–CS solution on the ethanol– acetic acid ratios.

The rheological properties of the solution vary greatly depending on the ratio of ethanol and acetic acid in the solution, where the pH value increases with the decreasing of acetic acid concentration, and the viscosity and conductivity values inconsistent change.

As mentioned above, the heterogeneous jump in viscosity η_0 is caused by two opposing trends in viscosity variations when acetic acid concentration decreases and ethanol concentration increases. The first one is that when the density of hydrogen bonds between acetic acid molecules and polymers reduces, so does the size of macromolecule blocks and viscosity. The second tendency is a drop of CS solubility due to an insufficient pH value for the CS polycation, which enhances the polymer's intermolecular stickiness and viscosity. As a result, the viscosity of PVA–CS solutions changed unevenly.

The electrical conductivity depends on the density of free ions and the viscosity of the solution and therefore also varies heterogeneously. However, in general, the conductivity of the solution decreases with increase of ethanol– acetic acid ratio.

The change of rheological properties leads to an adaptation in the ability to form nanofibers by electrospinning. In a previous study on the fabrication of PVA–CS nanofibers from the solution of 4% PVA and 3% CS without the presence of ethanol, the obtained nanofibers diameter was 326 ± 62 nm at the optimal needle–collector distance of 140 mm, feed rate of 0.1 mL/h and voltage of 27 kV [26]. It

 doi:10.20944/preprints202410.0296.v1

will be interested to investigate how the addition of ethanol to the electrospinning solution affects nanofibers production, electrospinning technology parameters, and the properties of the generated PVA CS nanofibers.

3.3. Effect of Ethanol– Acetic Acid Ratio on Fabrication of PVA–CS Nanofibers

3.3.1. The Ability to Fabricate PVA–CS Nanofibers

Solutions containing 4% PVA, 3% CS and 60% acetic acid and ethanol mixtures were electrospinning to investigate their ability to fabricate nanofibers. The influence of the technological parameters, including the distance between the needle tip and the collector being varied from 100 to 150 mm, the voltage being altered from 16 to 30 kV, and the flow rate being adjusted from 0.1–0.2 mL/h on the nanofibers fabrication is presented in Table 4.

Table 4. The ability of PVA–CS nanofiber fabrication at different concentrations of ethanol and acetic acid under electrospinning conditions: the needle–collector distance 100 – 150 mm, the feed rate 0.1 – 0.2 mL/h, the voltage 16 – 30 kV.

Distance (mm)	Feed rate (mL/h)	C_{CH_3COOH} (% w/w)	$C_{C_2H_5OH}$ (% w/w)	Voltage (kV)									
				16	18	20	22	24	26	27	28	29	30
150	0.1	60	0	O	O	o	+	+	+	+	+	+	+
		55	5	O	O	o	+	+	+	+	+	+	+
		50	10	O	O	o	+	+	+	+	+	+	+
		45	15	O	o	+	+	+	+	+	+	+	+
		40	20	O	o	+	+	+	+	+	+	+	+
	0.2	60	0	O	O	O	o	+	+	+	+	+	+
		55	5	O	O	o	o	+	+	+	+	+	+
		50	10	O	O	o	o	+	+	+	+	+	+
		45	15	O	O	o	+	+	+	+	+	+	+
		40	20	O	O	o	+	+	+	+	+	+	+
140	0.1	60	0	O	o	+	+	+	+	+	+	+	+
		55	5	O	O	o	+	+	+	+	+	+	+
		50	10	O	O	o	+	+	+	+	+	+	+
		45	15	O	o	+	+	+	+	+	+	+	+
		40	20	O	o	+	+	+	+	+	+	+	+
	0.2	60	0	O	O	O	o	+	+	+	+	+	+
		55	5	O	O	o	o	+	+	+	+	+	+
		50	10	O	O	o	*	+	+	+	+	+	+
		45	15	O	O	*	+	+	+	+	+	+	+
		40	20	O	O	o	+	+	+	+	+	+	+
120	0.1	60	0	O	o	+	+	+	+	+	+	+	+
		55	5	O	o	+	+	+	+	+	+	+	+
		50	10	O	o	+	+	+	+	+	+	+	+
		45	15	o	+	+	+	+	+	+	+	+	+
		40	20	o	o	+	+	+	+	+	+	+	+
	0.2	60	0	O	o	o	*	*	+	+	+	+	+

 doi:10.20944/preprints202410.0296.v1

		55	5	O	O	o	+	+	+	+	+	+	+
		50	10	O	O	o	+	+	+	+	+	+	+
		45	15	O	o	+	+	+	+	+	+	+	+
		40	20	O	o	o	+	+	+	+	+	+	+
		60	0	O	o	+	+	+	+	+	+	+	+
		55	5	O	o	+	+	+	+	+	+	+	+
	0.1	50	10	O	o	+	+	+	+	+	+	+	+
		45	15	o	+	+	+	+	+	+	+	+	+
		40	20	o	+	+	+	+	+	+	+	+	+
100		60	0	O	o	+	+	+	+	+	+	+	+
		55	5	O	o	*	+	+	+	+	+	+	+
	0.2	50	10	O	o	*	+	+	+	+	+	+	+
		45	15	o	*	+	+	+	+	+	+	+	+
		40	20	o	*	+	+	+	+	+	+	+	+

(+) the formation of fibers; *(O) the formation of droplets and a few fibers;*
(o) the formation of fibers and a few drops; *(*) the formation of fibers, but the process is unstable*

Thus, the PVA–CS nanofibers fabrication ability from the ethanol–acetic acid ratio of 15–45 is the greatest.

3.3.2. Intermolecular interactions for the PVA–CS nanofibers fabrication

The impact of intermolecular interactions between polymers and solvents as well as between polymers themselves on the acquired properties of polymer nanofibers is one of the most significant concerns related to the electrospinning process. According to Hildebrand-Scatchard theory, dispersion, polar, and hydrogen forces (f_d, f_p and f_h) make up intermolecular interactions, with the dispersion component counting for the majority of these interactions. The solubility parameters of the components approach each other as the molar enthalpy of mixing (ΔH) approaches zero. Figure 4 depicts a Teas diagram that accounts for each component's contribution (assuming that their sum equals 100%) and is based on the presumption that all materials are equal.

For every part of the experimental combination, dispersion forces (f_d), polar forces (f_p), and hydrogen bond forces (f_h) were calculated. Table 5 presents these fibers formation parameters.

In our previous work, the influence of acetic acid on the solubility parameters of a 4%PVA-3%CS solution was reported [26]. To better illustrate the differences in effects between the two solvent systems with and without ethanol, Figure 5 reconstructs the Teas diagram for both co-solvent systems.

Table 5. The parameters of fractional solubility in the solution of 4% PVA–3% CS in the mixture of solvents CH_3COOH-C_2H_5OH-H_2O.

CH_3COOH wt.%	**C_2H_5OH wt.%**	**H_2O wt.%**	**$100f_d$**	**$100f_p$**	**$100f_h$**	**f_h-f_p**	**f_h-f_d**	**f_p-f_d**
60	0	33	32,19	24,13	43,68	19,55	11,48	-8,06
55	5	33	31,98	23,91	44,11	20,19	12,13	-8,06
50	10	33	31,76	23,70	44,54	20,84	12,77	-8,06
45	15	33	31,55	23,48	44,97	21,48	13,42	-8,06
40	20	33	31,33	23,27	45,40	22,13	14,06	-8,06
35	25	33	31,12	23,05	45,83	22,77	14,71	-8,06

 doi:10.20944/preprints202410.0296.v1

Given that water makes up 33% of the mixtures in this experiment, it was possible to create a three-dimensional graph by the plotting of the concentrations of solely CH_3COOH and C_2H_5OH along the X and Y axes, while the values of f_d, f_p and f_h were drawn along the Z axis and (Figure 5).

Compared to the solution without ethanol, it is evident that the addition of ethanol to PVA-CS-CH_3COOH solutions has the effect of the stabilization of the parameters of 4% PVA–3% CS solutions.

Thus, it can be concluded that binary, trinary, or other multi-component solutions with a "f_h-f_p" value between 19.5 and 21.5% are appropriate for the use in the electrospinning process for PVA-CS nanofibers fabrication.

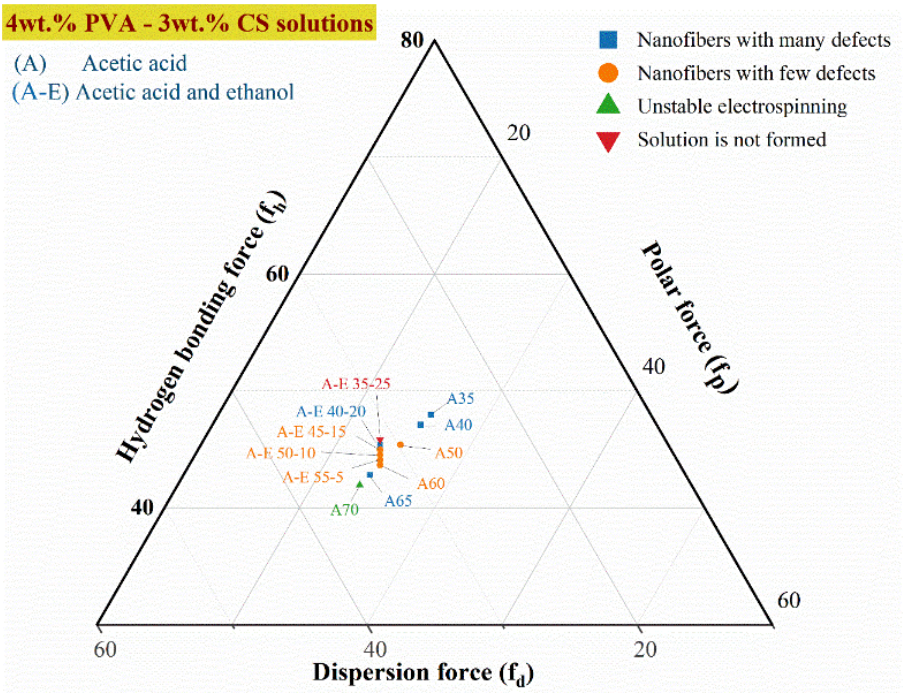

Figure 4. The Teas plot for PVA-CS electrospinning solutions with CH_3COOH-H_2O and CH_3COOH-C_2H_5OH-H_2O as the co-solvent system.

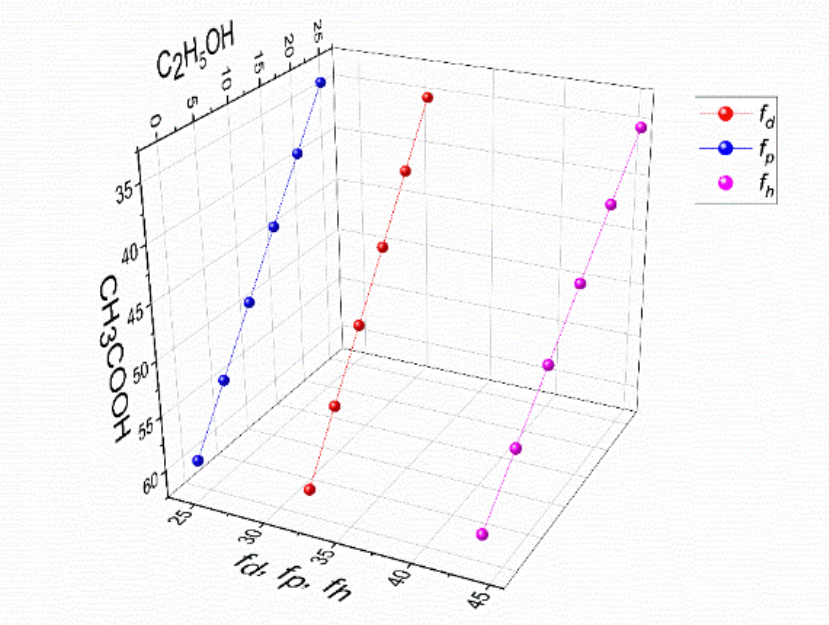

Figure 5. Values of polar interactions f_h, f_p, f_d for a mixture of solvents CH_3COOH-C_2H_5OH-H_2O in the solution of 4% PVA- 3% CS.

 doi:10.20944/preprints202410.0296.v1

3.3.3. Morphology of PVA–CS Nanofibers

Micrographs of nanofibers obtained from 4% PVA–3% CS–ethanol–acetic acid solutions with electrospinning parameters fixed at the needle–collector distance of 140 mm, the voltage 28 kV, the feed rate 0.2 mL/h were used to investigate the effect of ethanol–acetic acid ratios on the morphology and diameter of PVA–CS nanofibes.

From the data presented in Table 6 and on Figure 6 it can be concluded that the addition of ethanol to the electrospinning solution clearly altered the fabrication ability of PVA–CS nanofibers as well as their morphology and diameter. The results of microimage analysis and diameters of nanofibers obtained from solutions with different concentrations of ethanol–acetic acid revealed that the solution with ethanol-acetic acid ratio 15 – 45 has the lowest viscosity and is also the solution for high nanofiber fabrication capability with the finest morphology and the smallest diameter.

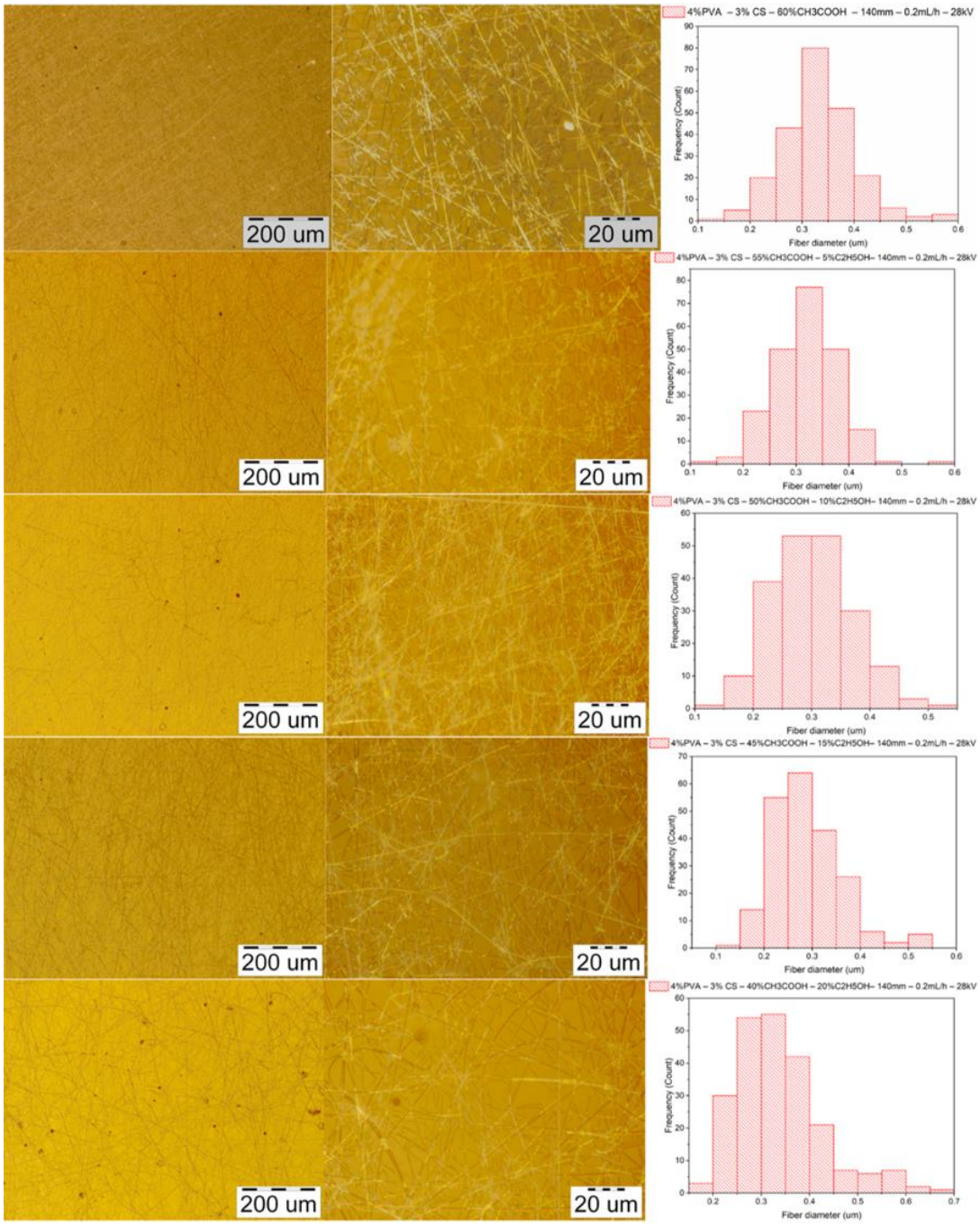

Figure 6. Microscopic images at 100x and 1000x and the diameter distributions of PVA–CS nanofibers obtained from solutions of 4% PVA, 3% CS and different concentration of acetic acid and ethanol

 doi:10.20944/preprints202410.0296.v1

(electrospinning parameters fixed at collector – the needle distance of 140 mm, the feed rate 0.2 mL / h, the voltage 28 kV).

Table 6. Diameter distributions of electrospun PVA nanofibers obtained from solutions of 4% PVA, 3% CS and the different ratios of acetic acid /ethanol with the fixing electrospinning parameters at collector – the needle distance of 140 mm, the feed rate 0.2 mL / h, the voltage 28 kV.

Diameter (nm)	C_2H_5OH/CH_3COOH ratio (% w/w)				
	0/60	**5/55**	**10/50**	**15/45**	**20/40**
Mean	330	320	301	285	337
Standard deviation	68	59	68	65	91
Min	134	147	110	121	170
Max	587	573	533	592	654

The observation of nanofibers formation in the electrospinning as well as the results of the analysis of the micrographs and the diameter distribution of the nanofibers from solutions with different ethanol– acetic acid ratios showed that the solution 4% PVA, 3% CS, 15% ethanol and 45% acetic acid were optimal for the fabrication of PVA–CS nanofibers. As a result, further investigation of electrospinning parameters is required to determine the optimal technological parameters.

3.4. Effect of Ethanol– Acetic Acid Ratio on Optimal Electrospinning Parameters

3.4.1. Parameter of the Distance between the Needle Tip and the Collector

Electrospinning was performed with the solution of PVA–CS ratio 4–3 with the solvent ratio of ethanol– acetic acid 15–45, with the distance between the needle and the collector varying from 100 to 150 mm and the voltage and the speed fixed at 28 kV and 0.2 mL/h, respectively.

Figure 7 and Table 7 show microimages and statistics on fiber diameter distribution. The data demonstrate that the optimal distance between the needle and the collector for electrospinning is 140 mm. At this parameter, the fibrous film has the least number of defects, as well as the diameter of the resulting fibers is also the smallest.

Table 7. Diameter distribution of of PVA–CS nanofibers obtained from the solution of PVA–CS ratio 4–3 with the solvent ratio of ethanol– acetic acid 15–45 at the feed rate 0.2 mL/ h, the voltage 28 kV and variation of the needle–collector distance.

Diameter (nm)	Needle–collector distance (mm)				
	100	**120**	**130**	**140**	**150**
Mean	313	302	295	285	308
Standard deviation	77	75	70	65	76
Min	139	124	124	121	155
Max	646	562	546	592	540

 doi:10.20944/preprints202410.0296.v1

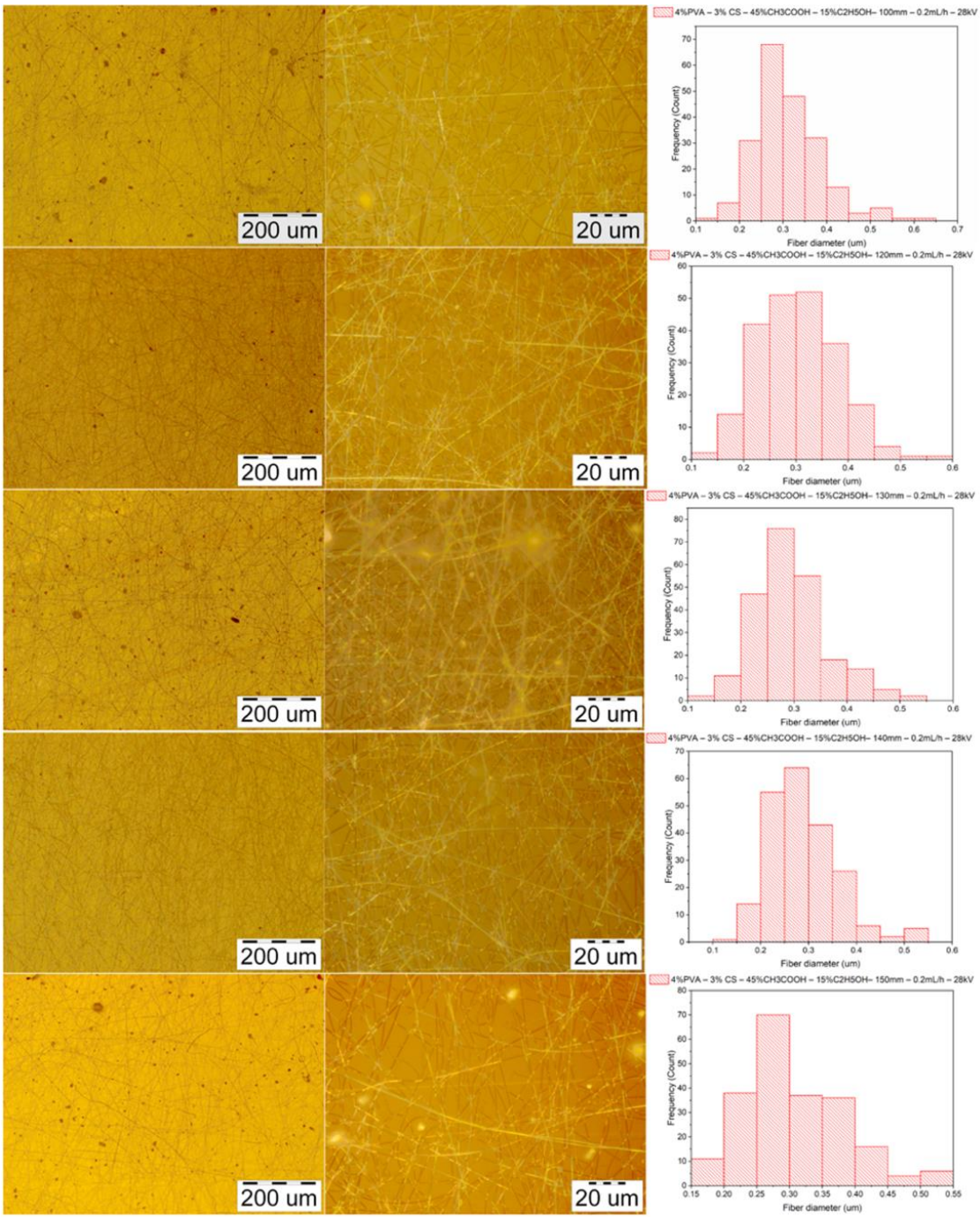

Figure 7. Microscopic images at 100x and 1000x and diameter distributions of PVA–CS nanofibers obtained from the solution of PVA–CS ratio 4–3 with the solvent ratio of ethanol– acetic acid 15–45 at the feed rate 0.2 mL/h, the voltage 28 kV and variation of the needle–collector distance.

3.4.2. Parameters of Feed Rate

The solution of PVA–CS (ratio 4–3) with ethanol–acetic acid solvent (ratio 15–45) was electrospun with the voltage and the needle–collector distance fixed at 28 kV and 140 mm, respectively, and the rate was adjusted from 0.1 mL/h to 0.4 mL/h. Microimages and fibers diameter distribution statistics are shown on Figure 8 and in Table 8.

 doi:10.20944/preprints202410.0296.v1

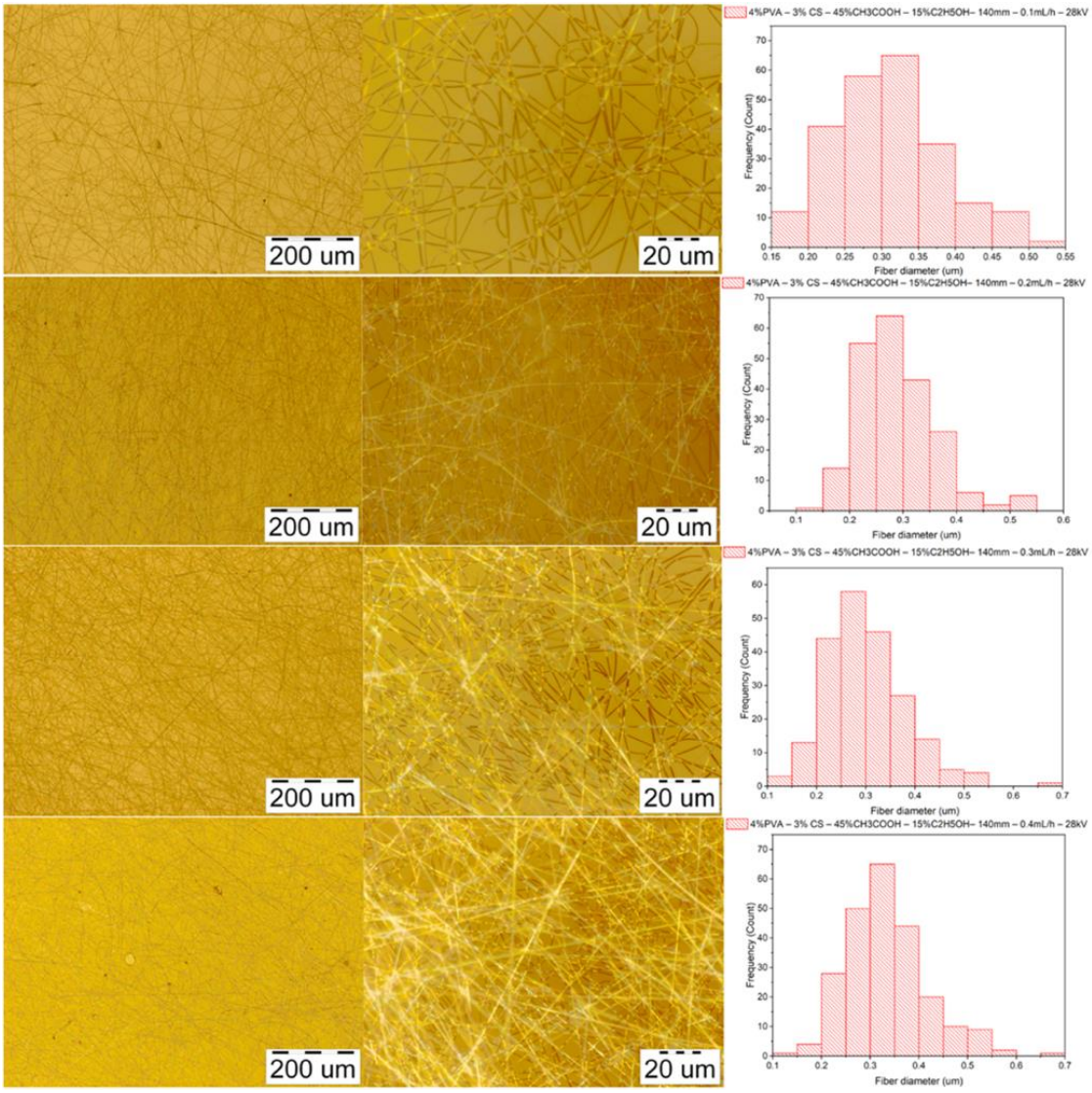

Figure 8. Microscopic images at 100x and 1000x and diameter distributions of PVA–CS nanofibers obtained from solution of PVA–CS ratio 4–3 with a solvent ratio of ethanol– acetic acid 15–45 at the needle–collector distance 140 mm, the voltage 28 kV and variation of the feed rate from 0.1 to 0.4 mL/ h.

Table 8. Diameter distribution of PVA–CS nanofibers obtained from the solution of PVA–CS ratio 4–3 with the solvent ratio of ethanol– acetic acid 15–45 at the needle–collector distance 140 mm, the voltage 28 kV and variation of the feed rate from 0.1 to 0.4 mL/ h.

Diameter (nm)	**Feed rate (mL/h)**			
	0.1	**0.2**	**0.3**	**0.4**
Mean	311	285	300	335
Standard deviation	75	65	79	83
Min	154	121	134	131
Max	513	592	670	650

Thus, at the needle–collector distance parameters of 140 mm, the feed rate of 0.2 mL/h and the voltage of 28 kV the PVA–CS nanofibers obtained have the smallest diameter of 285 ± 65 nm. At the feed rate of 0.3 mL/h although the PVA–CS nanofibers have less defects, the fiber diameter is larger.

 doi:10.20944/preprints202410.0296.v1

3.4.3. Parameters of the Voltage

The solution of PVA–CS (the ratio 4–3) with the solvent ratio of ethanol-acetic acid 15–45 was subjected to electrospinning with the fixed distance between the needle and the collector of 140 mm, the flow rate set at 0.2 mL/h, and the voltage change between 25 kV and 30 kV. Microscopic images and fiber diameters distribution statistics are shown on Figure 9 and in Table 9.

The morphological analysis and diameter distribution of PVA–CS nanofibers revealed that at 28 kV, the obtained fibers had the smallest diameter with fewest defects. The optimal technological parameters for the electrospinning include the needle–collector distance of 140 mm, the feed rate of 0.2 mL/h and the voltage of 28 kV. The obtained PVA–CS nanofibers have the diameter of 285 ± 65 nm.

Table 9. Diameter dibstribution of PVA–CS nanofibers obtained from solution of PVA–CS (ratio 4–3) with the solvent ratio of ethanol– acetic acid 15–45 at the needle–collector distance 140 mm, the feed rate 0.3 mL/ h and the variation of voltage from 25 to 30 kV.

Diameter (nm)	**Voltage (kV)**					
	25	**26**	**27**	**28**	**29**	**30**
Mean	348	334	309	285	307	318
Standard deviation	102	99	91	65	96	114
Min	97	139	110	121	131	120
Max	652	734	600	592	644	689

The fabrication of PVA–CS nanofibers without ethanol leads to the nanofiber diameter 326 ± 62 nm, and the optimal feed rate was only 0.1 mL/h. When compared to the acetic acid, the mixed solvent of 45% acetic acid and 15% ethanol not only improved the morphology and diameter of PVA–CS nanofibers, but also doubled or tripled the nanofiber fabrication yield (at the feed rate 0.3 mL/h diameter was 300 ± 79 nm).

 doi:10.20944/preprints202410.0296.v1

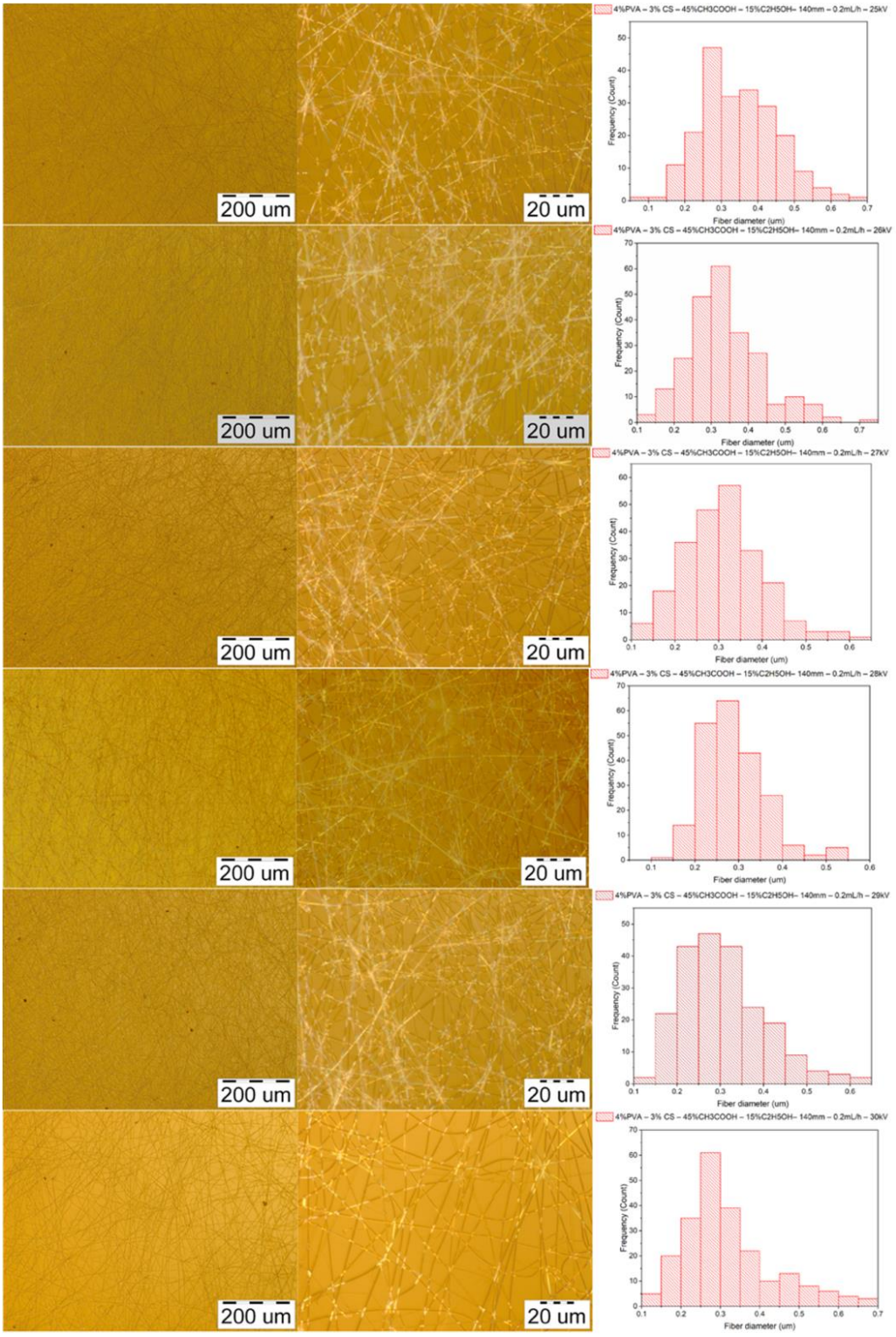

Figure 9. Microscopic images at 100x and 1000x and diameter distributions of PVA–CS nanofibers obtained from the solution of PVA–CS (ratio 4–3) with the solvent ratio of ethanol– acetic acid 15–45 at the needle–collector distance 140 mm, the feed rate 0.3 mL/ h and the variation of voltage from 25 to 30 kV.

3.5. Fourier–Transform Infrared (FTIR) Spectroscopy

In our previous research [26] it was established that acetic acid entirely separates from the nanofiber matrix and has no effect on the polymeric components of PVA–CS nanofiber. Infrared

 doi:10.20944/preprints202410.0296.v1

spectra of nanofibers fabricated from the solutions of PVA–CS and ethanol–acetic acid in different rations were taken in order to analyze the effect of ethanol on the chemical bonds formation in the system of PVA–CS nanofibers.

Infrared spectra of PVA–CS nanofibers (Figure 10) demonstrated that they are the same. The peak positions did not change, indicating that no new chemical bonds were formed when ethanol was added to the electrospinning solution system. Thus, it is evident that during electrospinning, ethanol and acetic acid were entirely separated from the PVA–CS nanofiber mat.

When two polymers are combined in the PVA–CS nanofibers, the IR spectra of the nanofiber systems become simpler and closely resemble that of pure PVA. The oscillations of the C–H alkyl bond in the CS molecule at 2869 cm^{-1} [32] take on a shoulder shape when combined with the asymmetric and symmetric stretching bands of the CH_2 groups in the PVA molecule at 2940 cm^{-1} and 2910 cm^{-1} [33,34]. In the PVA–CS nanofibers, the bands of each polymer in the 1590–890 cm^{-1} region become simpler, wider, less multiple, and shift into the space between bands. These are evidences that PVA and CS are closely linked together in the PVA–CS nanofiber system.

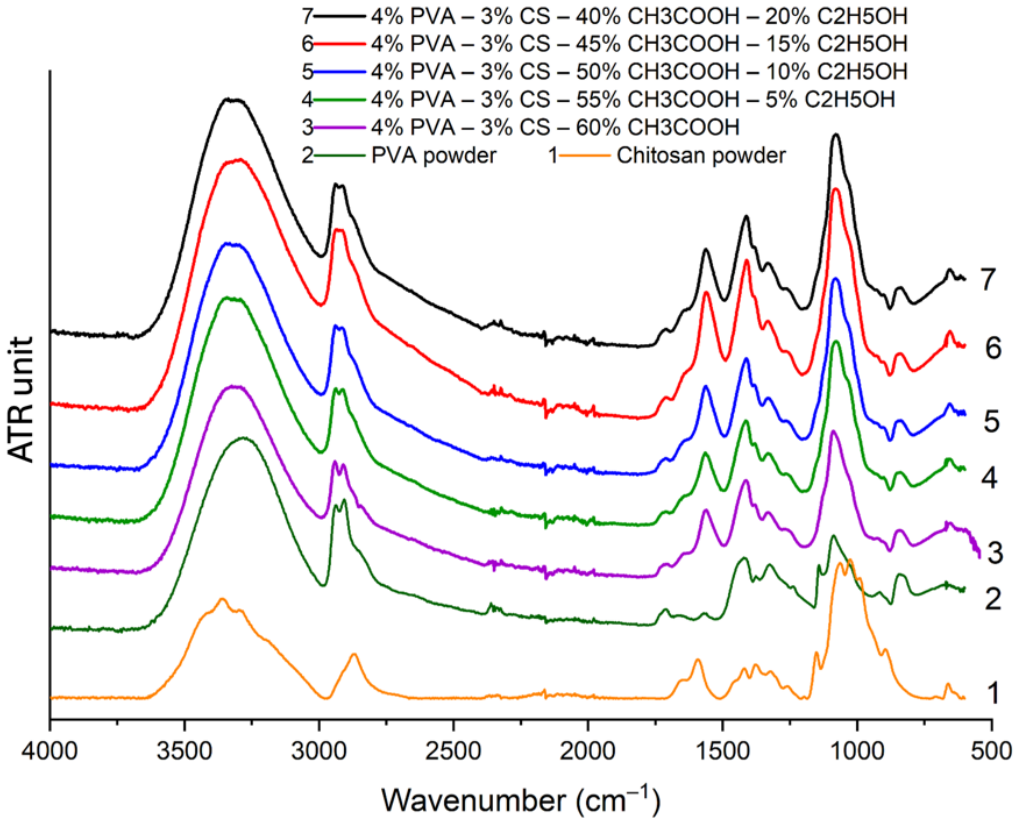

Figure 10. Infrared spectra of PVA powder, chitosan powder and PVA–CS nanofibers.

There was a combination of bands at 3279 cm^{-1} (of -OH bonds in PVA molecule), 3300 cm^{-1} and 3362 cm^{-1} (of -OH and -NH bonds in CS molecule) to form a broad and high intensity band in the region of 3000–3600 cm^{-1} common to all -OH and -NH groups in the polymer system [32–35]. The 896 cm^{-1} band of the -OH out–of–plane vibrations and the 690 cm^{-1} band of the N–H twist vibrations related to ring stretching in the IR spectrum of CS disappeared in the nanofibers spectra, demonstrating mobility of the -OH and $-NH_2$ groups of CS are disappeard [36–38]. The disappearance of these mobilities, together with the broadening of the absorption region in the range 3000–3600 cm^{-1}, suggests that significant number of hydrogen bonds formed between the PVA and CS molecules. The similar conclusions were made in the previous publications [34,35].

 doi:10.20944/preprints202410.0296.v1

3.6. X–ray diffraction (XRD) Analysis

The XRD spectral data are shown on Figure 11 and the results on the crystal lattice parameters of the obtained nanofiber systems are presented in Table 10.

Overall, compared to the polymer powders, the XRD spectra of the PVA and PVA–CS nanofibers have stronger and more noticeable peaks. As PVA was converted from a powder to nanofiber, the position and intensity of its peaks altered significantly. The PVA–CS nanofibers' XRD peak intensities varied slightly from those of the PVA nanofibers and from each other, indicating that solvent factors in addition to the presence of CS and the powder–to–nanofiber transitions affect the crystal structure of these nanofibers.

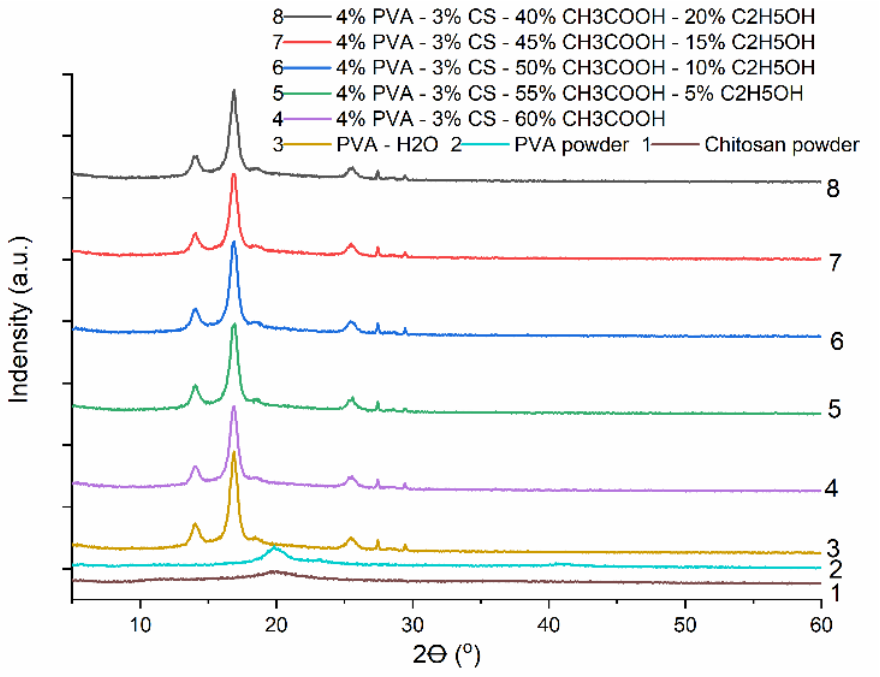

Figure 11. X–Ray diffraction of PVA powder, CS powder, PVA nanofibers from aqueous solution and PVA – CS nanofibers from aqueous solution with C_2H_5OH and CH_3COOH.

Table 10. The lattice parameters of PVA–CS nanofibers obtained from electrospun solutions with different ethanol– acetic acid ratios.

Lattice parameters		Axial Lengths [Å]			Angles [°]			Cell volume [Å³]	Crystal-linity (%)
		a	b	c	α	β	γ		
Powder	CS	15.7371	8.3352	3.0609	90	90	90	401.5017	48.29
	PVA	15.2596	5.2416	9.7092	90	97.188	90	770.4844	57.69
Ethanol–acetic acid	0–60	12.6928	3.5873	10.8013	90	95.237	90	489.7613	60.64
	5–55	7.6994	16.7927	6.8328	90	96.878	90	877.0803	54.64
	10–50	15.9762	5.5865	9.3954	90	93.823	90	836.6833	62.36
	15–45	12.7499	7.2561	8.637	90	92.457	90	798.3136	57.45
	20–40	16.0564	4.1401	11.3214	90	93.814	90	750.9244	52.22

The results (Table 10) revealed that the increasing of the ethanol concentration and the decreasing of the acetic acid concentration in the initial electrospinning solution caused a unit cell volume reduction in the PVA–CS nanofibers lattice. However, in the absence of ethanol, the volume of the lattice unit cell is the smallest.

 doi:10.20944/preprints202410.0296.v1

The crystallinity of the nanofiber systems as well as the axial lengths of the irregularly varied crystal cells can be derived from the irregular variation of the viscosity and electrical conductivity of the original solutions.

The variation in crystal structure implies that the ethanol and acetic acid components in the initial electrospun solution also have an impact on the mechanical and thermal properties of the produced PVA–CS nanofiber systems.

3.7. Differential Scanning Calorimetry (DSC) Analysis

Information about the DSC curves of PVA–CS nanofibers that were electrospun from polymer solutions at different solvent ratios is shown on Figure 12 and in Table 11.

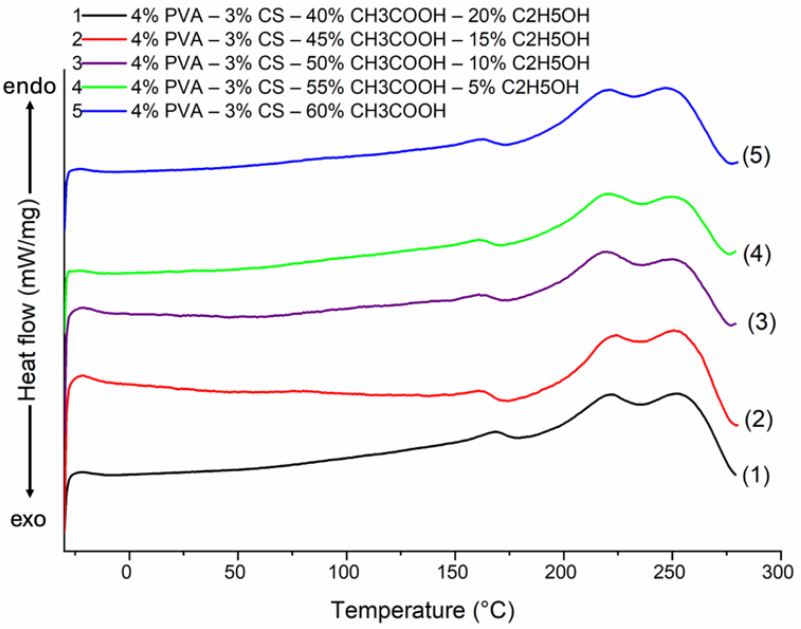

Figure 12. DSC heating curve of PVA–CS nanofibers at different ethanol– acetic acid ratios.

The enthalpy change (ΔH), crystallinity (χ), melting temperature (T_m), and glass transition temperature (T_g) results for PVA–CS nanofibers at the different ethanol– acetic acid ratio in electrospinning solutions are presented in Table 11.

Table 11. DSC data for the thermal desorption of PVA – CS nanofibers at the different ethanol– acetic acid ratio in electrospinning solutions.

Ethanol– acetic acid ratio	ΔH_{PVA} (J/g)	χ_{PVA} (%)	ΔH_{CS} (J/g)	T_g (°C)	T_m(°C)
0–60	57.22	38.15	5.86	75	222, 247
5–55	42.23	28.15	11.19	75	220, 249
10–50	44.09	29.39	9.79	84	220, 250
15–45	38.72	25.81	13.82	75	222, 251
20–40	53.73	35.82	2.56	87	223, 252

The DSC heating curves of PVA–CS nanofibers at the various ethanol– acetic acid ratios are slightly different. Specifically, as the percentage of ethanol increases, both the crystallization temperature and the melting point increase slightly. This indicates that the different solvent ratios had an effect on the linking intensity of the polymers during electrospinning procedure.

There is the correlation between both the results presented in Table 11 and those in Table 1 and on Figure 1. The change of the specific enthalpy of PVA on the DSC curve of PVA-CS nanofibers was

 doi:10.20944/preprints202410.0296.v1

decreased when the optical density (*A*) and turbidity of the solution dropped (at acetic acid-ethanol ratios of 55-5, 50-10, and 45-15). This suggests that the aggregation state of polymer macromolecules in the initial solution influences polymer crystallization during the electrospinning.

The reduction of ΔH_{PVA} by about 20-30% while ΔH_{CS} increased by 2-fold suggests that the enhancement of the ethanol ratio in the initial solution mainly affects the structure of CS macromolecules rather than the PVA macromolecules.

Thus, an alteration of the ethanol-acetic acid ratio in the initial solution results in a change in the polymer's aggregation state in the initial solution, which leads to an adjustment of the individual crystal composition of each polymer in the structure of the PVA-CS nanofiber system. This results in a modification in the lattice, which affects the overall crystallinity of the system. In general, increasing the proportion of ethanol decreases the volume of the unit cell in the crystal lattice and raises the temperature of crystallization and melting of the system.

3.8. Thermogravimetric Analysis (TGA)

TGA curves for heating PVA powder, CS powder, and PVA–CS nanofibers at the different solvent ratios are shown in Figure 13.

PVA powder and PVA nanofibers path through three basic stages of heat degradation, whereas CS powder only goes through two. The main stage of the CS powder decomposes at a higher temperature than the other samples, demonstrating that the CS molecules are more heat resistant due to their intricate structure. However, as a result of that, almost all CS bonds breakdown during this stage.

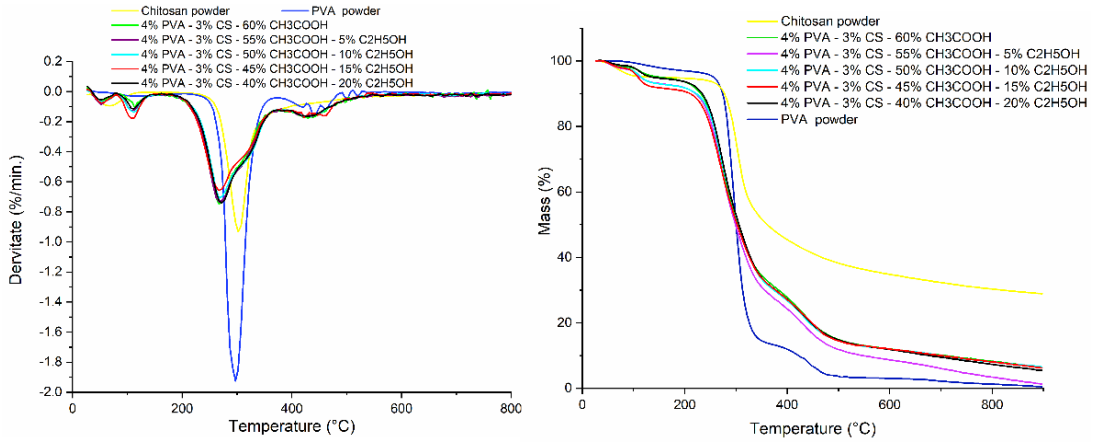

Figure 13. TGA thermogram of PVA powder, CS powder and PVA–CS nanofibers at different ethanol– acetic acid ratios in initial electrospun solution.

Table 12. The stages of thermal decomposition and weight reduction of powder and nanofibers samples.

Degradation stages		Powder		PVA–CS nanofibers with different CH_3COOH/C_2H_5OH ratios				
		PVA	CS	60 – 0	55 – 5	50 – 10	45 – 15	40 – 20
First stage	Range (°C)	25–202	25–177	25–172	25–172	25–172	25–172	25–172
	Peaks (°C)	112	67	52; 114	52; 112	52; 112	52; 107	52; 112
	Weight loss (%)	3.04	5.21	5.42	7.34	5.63	8.58	5.63

 doi:10.20944/preprints202410.0296.v1

Second stage	Range (°C)	202–367	177–462	172–377	172–377	172–377	172–377	172–377
	Peaks (°C)	297	302	267	272	272	267	272
	Weight loss (%)	83.37	77.04	63.79	64.19	62.94	61.40	64.31
Third stage	Range (°C)	367–527		377–547	377–547	377–547	377–547	377–547
	Peaks (°C)	422; 442; 462		429; 459	422; 437	427	422; 437; 457	427
	Weight loss (%)	10.32		17.64	18.43	16.72	16.97	16.97

PVA–CS nanofibers' thermal degradation process resembles a coherence of the thermal decomposition of the two polymers. This again confirms that following the electrospinning procedure, the solvents were virtually entirely removed from the nanofiber system. The decomposition temperatures of these nanofibers, on the other hand, were all lower than those of pure polymers, indicating that their complexes were formed by weak bonds.

Thus, the change of the ethanol–acetic acid ratio has no effect on the thermal decomposition of the PVA–CS nanofibers.

3.9. Tensile Property

The vertical and horizontal tensile properties of PVA–CS nanofiber matrices prepared from 4% PVA, 3% CS, and different ethanol/acetic acid ratios were investigated (Table 13, Figures 13 and 14).

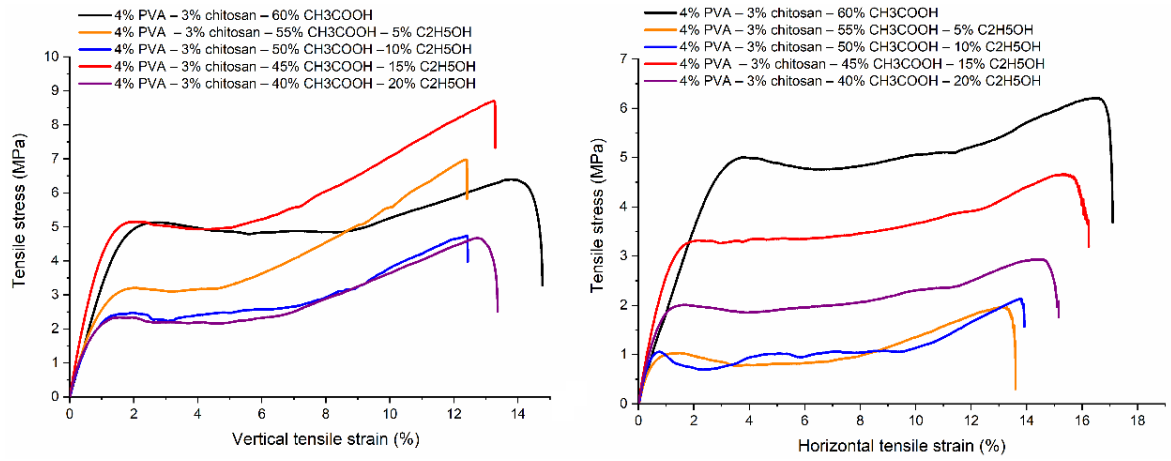

Figure 14. The deformation of PVA–CS nanofibers according to the ethanol–acetic acid ratios in the electrospun sulutions.

Table 13. Parameters of tensile properties of PVA–CS nanofibers.

Ethanol– acetic acid ratio	Tensile strength [MPa]		Elongation at Break [%]		Young's modulus [MPa]	
	Vertical	*Horizontal*	*Vertical*	*Horizontal*	*Vertical*	*Horizontal*
0–60	5.937 ± 1.046	5.673 ± 0.560	14.05 ± 1.75	17.06 ± 0.47	343.532 ± 33.840	289.180 ± 74.027

 doi:10.20944/preprints202410.0296.v1

5–55	5.594 ± 1.501	1.617 ± 0.416	12.12 ± 1.64	13.27 ± 1.10	424.921 ± 72.966	246.112 ± 34.894
10–50	4.732 ± 0.457	1.900 ± 0.450	11.80 ± 1.48	13.97 ± 2.14	427.543 ± 50.422	270.074 ± 40.440
15–45	7.916 ± 0.970	4.912 ± 0.965	13. 07 ± 0.53	16.40 ± 0.82	546.113 ± 32.150	333.086 ± 23.851
20–40	4.536 ± 0.918	2.893 ± 0.220	12.69 ± 1.96	14.10 ± 1.90	398.311 ± 47.879	329.703 ± 29.510

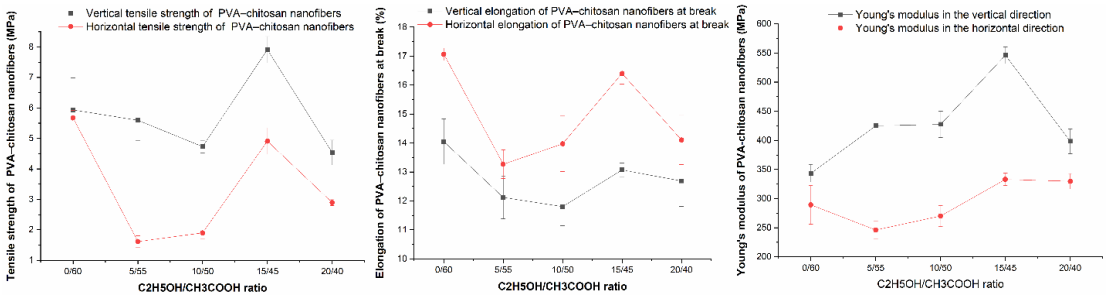

Figure 15. Changes in tensile properties of PVA–CS nanofibers according to ethanol–acetic acid ratios in the electrospun solutions.

Each sample has a vertical tensile strength and Young's modulus that are greater than their horizontal counterparts, as well as a vertical elongation at break that is smaller than a horizontal.

Similar to the change in the rheological properties of PVA–CS solutions in acetic acid and ethanol solutions, it is evident that there is no discernible pattern in the variation of the samples' tensile characteristics.

Compared to the PVA–CS nanofibers from the ethanol–free solution, the PVA–CS nanofibers obtained with an ethanol–acetic acid (ratio of 15–45), the vertical tensile strength increased by 33%, the horizontal tensile strength decreased by 12% , the elongation at break reduced by 1% and the vertical and horizontal Young's modulus improved by 59% and 15% respectively.

4. Conclusions

For the first time, ethanol was used in the electrospinning solution of PVA-CS and showed encouraging effects for the improving of the morphology and fabrication yield of PVA-CS nanofibers.

The usage of ethanol and acetic acid demonstrates the effect of shifting the solvent system's solubility parameters, changing the interaction of the different component forces in the solution, and therefore producing significant effects on the optical and rheological properties of PVA-CS solution.

To summarize, using an ethanol–acetic acid ratio of 15–45 in the PVA–CS solution resulted in the following outcomes:

- improved the morphology, diameter, and manufacturing productivity of PVA–CS nanofibers by 2–3 times due to the reduction of defects, reducing the diameter of nanofibers from 326 ± 62 nm (0.1 mL/h without ethanol) to 285 ± 65 nm (0.2 mL/h) or 300 ± 79 nm (0.3 mL/h);
- did not change the chemical nature of the resulting system of nanofibers, thereby maintaining the thermal properties of the PVA–CS nanofiber system;
- changed the structure of the crystal lattice of the nanofibers, which leads to a modification in the mechanical properties of the nanofibers. The PVA–CS nanofibers appear to become stronger by the increasing of the vertical tensile strength by 33%, the increasing of the vertical and horizontal Young's moduli by 59% and 15%, and the reducing of the elongation at break by 1%.

Besides, usually the use of multi–component solvent system had the effect of expanding the solubility of organic compounds in general and biologically active materials in particular. In this

 doi:10.20944/preprints202410.0296.v1

instance, using a reasonable ethanol–acetic acid ratio resulted in a decrease of the viscosity of the PVA–CS solution, which creates the possibility for the increasing of the drug amount in the solution.

Author Contributions: Conceptualization, T.H.N.V., S.N.M. and A.V.P.; methodology, T.H.N.V., M.V.U.; software, T.H.N.V.; validation, T.H.N.V., A.V.P. and S.N.M.; formal analysis, T.H.N.V.; investigation, T.H.N.V.; resources, R.O.O.; data curation, T.H.N.V.; writing—original draft preparation, T.H.N.V.; writing—review and editing, S.N.M.; visualization, T.H.N.V; supervision, M.V.U.; project administration, M.V.U.; funding acquisition, M.V.U. All authors have read and agreed to the published version of the manuscript.

Funding: The research was funded under the strategic academic leadership program "Priority 2023" (Agreement 075-15-2023-380 dated 20.02.2023).

Institutional Review Board Statement: Not applicable.

Data Availability Statement: The data presented in this work are available on request from the corresponding authors.

Conflicts of Interest: The authors declare no conflicts of interest.

References

1. Teodorescu, M.; Bercea, M.; Morariu, S. Biomaterials of PVA and PVP in Medical and Pharmaceutical Applications: Perspectives and Challenges. *Biotechnol Adv* 2019, *37*, 109–131, doi:https://doi.org/10.1016/j.biotechadv.2018.11.008.
2. DeMerlis, C.C.; Schoneker, D.R. Review of the Oral Toxicity of Polyvinyl Alcohol (PVA). *Food Chem Toxicol* 2003, *41*, 319–326, doi:10.1016/s0278-6915(02)00258-2.
3. Iqbal, D.N.; Tariq, M.; Khan, S.M.; Gull, N.; Sagar Iqbal, S.; Aziz, A.; Nazir, A.; Iqbal, M. Synthesis and Characterization of Chitosan and Guar Gum Based Ternary Blends with Polyvinyl Alcohol. *Int J Biol Macromol* 2020, *143*, 546–554, doi:10.1016/j.ijbiomac.2019.12.043.
4. Nataraj, D.; Reddy, R.; Reddy, N. Crosslinking Electrospun Poly (Vinyl) Alcohol Fibers with Citric Acid to Impart Aqueous Stability for Medical Applications. *Eur Polym J* 2020, *124*, 109484, doi:10.1016/j.eurpolymj.2020.109484.
5. Pervez, M.N.; Stylios, G.K.; Liang, Y.; Ouyang, F.; Cai, Y. Low-Temperature Synthesis of Novel Polyvinylalcohol (PVA) Nanofibrous Membranes for Catalytic Dye Degradation. *J Clean Prod* 2020, *262*, 121301, doi:10.1016/j.jclepro.2020.121301.
6. Muppalaneni, S.; Omidian, H. Polyvinyl Alcohol in Medicine and Pharmacy: A Perspective. *J Dev Drugs* 2013, *02*, 1–5, doi:10.4172/2329-6631.1000112.
7. Lizardi-Mendoza, J.; Argüelles Monal, W.M.; Goycoolea Valencia, F.M. Chapter 1 - Chemical Characteristics and Functional Properties of Chitosan. In; Bautista-Baños, S., Romanazzi, G., Jiménez-Aparicio, A.B.T.-C. in the P. of A.C., Eds.; Academic Press: San Diego, 2016; pp. 3–31 ISBN 978-0-12-802735-6.
8. Aam, B.B.; Heggset, E.B.; Norberg, A.L.; Sørlie, M.; Vårum, K.M.; Eijsink, V.G.H. Production of Chitooligosaccharides and Their Potential Applications in Medicine. *Mar Drugs* 2010, *8*, 1482–1517, doi:10.3390/md8051482.
9. Gajra, B.; Pandya, S.S.; Vidyasagar, G.; Rabari, H.; Dedania, R.R.; Rao, S. Poly Vinyl Alcohol Hydrogel and Its Pharmaceutical and Biomedical Applications: A Review. *International Journal of Pharmaceutical Research* 2012, *4*, 20–26.
10. Kita, M.; Ogura, Y.; Honda, Y.; Hyon, S.-H.; Cha, W.-I.; Ikada, Y. Evaluation of Polyvinyl Alcohol Hydrogel as a Soft Contact Lens Material. *Graefe's Archive for Clinical and Experimental Ophthalmology* 1990, *228*, 533–537, doi:10.1007/BF00918486.
11. Jiang, Y.; Schädlich, A.; Amado, E.; Weis, C.; Odermatt, E.; Mäder, K.; Kressler, J. In-Vivo Studies on Intraperitoneally Administrated Poly(Vinyl Alcohol). *J Biomed Mater Res B Appl Biomater* 2010, *93B*, 275–284, doi:https://doi.org/10.1002/jbm.b.31585.
12. Zairy, H. M. Ibrahim, E.M.R.E.-Z. Chitosan as a Biomaterial — Structure, Properties, and Electrospun Nanofibers, Concepts, Compounds and the Alternatives of Antibacterials. *Varaprasad Bobbarala, IntechOpen* 2015, 81–101, doi:10.5772/61300.

13. Martău, G.A.; Mihai, M.; Vodnar, D.C. The Use of Chitosan, Alginate, and Pectin in the Biomedical and Food Sector-Biocompatibility, Bioadhesiveness, and Biodegradability. *Polymers (Basel)* 2019, *11*, 1837, doi:10.3390/polym11111837.
14. Koltai, T. Cancer: Fundamentals behind PH Targeting and the Double-Edged Approach. *Onco Targets Ther* 2016, *9*, 6343–6360, doi:10.2147/OTT.S115438.
15. You, J.S.; Jones, P.A. Cancer Genetics and Epigenetics: Two Sides of the Same Coin? *Cancer Cell* 2012, *22*, 9–20, doi:10.1016/j.ccr.2012.06.008.
16. Lu, Y.; Aimetti, A.A.; Langer, R.; Gu, Z. Bioresponsive Materials. *Nat Rev Mater* 2016, *2*, 16075, doi:10.1038/natrevmats.2016.75.
17. Le, W.; Chen, B.; Cui, Z.; Liu, Z.; Shi, D. Detection of Cancer Cells Based on Glycolytic-Regulated Surface Electrical Charges. *Biophys Rep* 2019, *5*, 10–18.
18. Cascone, M.G.; Maltinti, S.; Barbani, N.; Laus, M. Effect of Chitosan and Dextran on the Properties of Poly(Vinyl Alcohol) Hydrogels. *J Mater Sci Mater Med* 1999, *10*, 431–435, doi:10.1023/A:1008983215833.
19. Li, L.; Hsieh, Y.-L. Chitosan Bicomponent Nanofibers and Nanoporous Fibers. *Carbohydr Res* 2006, *341*, 374–381, doi:https://doi.org/10.1016/j.carres.2005.11.028.
20. Sanchez-Alvarado, D.I.; Guzmán-Pantoja, J.; Páramo-García, U.; Maciel-Cerda, A.; Martínez-Orozco, R.D.; Vera-Graziano, R. Morphological Study of Chitosan/Poly (Vinyl Alcohol) Nanofibers Prepared by Electrospinning, Collected on Reticulated Vitreous Carbon. *Int J Mol Sci* 2018, *19*, 1718, doi:10.3390/ijms19061718.
21. Lu, S.; Tao, J.; Liu, X.; Wen, Z. Baicalin-Liposomes Loaded Polyvinyl Alcohol-Chitosan Electrospinning Nanofibrous Films: Characterization, Antibacterial Properties and Preservation Effects on Mushrooms. *Food Chem* 2022, *371*, 131372, doi:10.1016/j.foodchem.2021.131372.
22. Bazzi, M.; Shabani, I.; Mohandesi, J.A. Enhanced Mechanical Properties and Electrical Conductivity of Chitosan/Polyvinyl Alcohol Electrospun Nanofibers by Incorporation of Graphene Nanoplatelets. *J Mech Behav Biomed Mater* 2022, *125*, 104975, doi:10.1016/j.jmbbm.2021.104975.
23. Gupta, S.; Pramanik, A.K.; Kailath, A.; Mishra, T.; Guha, A.; Nayar, S.; Sinha, A. Composition Dependent Structural Modulations in Transparent Poly(Vinyl Alcohol) Hydrogels. *Colloids Surf B Biointerfaces* 2009, *74*, 186–190, doi:10.1016/j.colsurfb.2009.07.015.
24. BUNN, C.W. Crystal Structure of Polyvinyl Alcohol. *Nature* 1948, *161*, 929–930, doi:10.1038/161929a0.
25. British Standards Institution. Plastics. Part 3. Test Conditions for Films and Sheets. : Determination of Tensile Properties.; BSI, 1996; ISBN 0580249824.
26. Vu, T.H.N.; Morozkina, S.N.; Sitnikova, V.E.; Olekhnovich, R.O.; Podshivalov, A. V.; Uspenskaya, M. V. A Systematic Investigation of Solution and Technological Parameters for the Fabrication and Characterization of Poly (Vinyl Alcohol) –Chitosan Electrospun Nanofibers. *Polym Adv Technol* 2024, *35*, doi:10.1002/pat.6423.
27. Bohren, C.F. and H.D.R. Absorption and Scattering of Light by Small Particles. *John Wiley and Sons, Inc.* 1998, 544.
28. Haiss, W.; Thanh, N.T.K.; Aveyard, J.; Fernig, D.G. Determination of Size and Concentration of Gold Nanoparticles from UV−Vis Spectra. *Anal Chem* 2007, *79*, 4215–4221, doi:10.1021/ac0702084.
29. Doak, J.; Gupta, R.K.; Manivannan, K.; Ghosh, K.; Kahol, P.K. Effect of Particle Size Distributions on Absorbance Spectra of Gold Nanoparticles. *Physica E Low Dimens Syst Nanostruct* 2010, *42*, 1605–1609, doi:10.1016/j.physe.2010.01.004.
30. Byron Bird, R.; Carreau, P.J. A Nonlinear Viscoelastic Model for Polymer Solutions and Melts—I. *Chem Eng Sci* 1968, *23*, 427–434, doi:10.1016/0009-2509(68)87018-6.
31. Cross, M.M. Rheology of Non-Newtonian Fluids: A New Flow Equation for Pseudoplastic Systems. *J Colloid Sci* 1965, *20*, 417–437, doi:10.1016/0095-8522(65)90022-X.
32. Miya, M.; Iwamoto, R.; Mima, S. FT-IR Study of Intermolecular Interactions in Polymer Blends. *Journal of Polymer Science: Polymer Physics Edition* 1984, *22*, 1149–1151, doi:10.1002/pol.1984.180220615.
33. Krimm, S.; Liang, C.Y.; Sutherland, G.B.B.M. Infrared Spectra of High Polymers. V. Polyvinyl Alcohol. *Journal of Polymer Science* 1956, *22*, 227–247, doi:10.1002/pol.1956.1202210106.
34. Koosha, M.; Mirzadeh, H. Electrospinning, Mechanical Properties, and Cell Behavior Study of Chitosan/PVA Nanofibers. *J Biomed Mater Res A* 2015, *103*, 3081–3093, doi:10.1002/jbm.a.35443.
35. Zheng, H.; Du, Y.; Yu, J.; Huang, R.; Zhang, L. Preparation and Characterization of Chitosan/Poly(Vinyl Alcohol) Blend Fibers. *J Appl Polym Sci* 2001, *80*, 2558–2565, doi:https://doi.org/10.1002/app.1365.

36. Vino, A.B.; Ramasamy, P.; Shanmugam, V.; Shanmugam, A. Extraction, Characterization and in Vitro Antioxidative Potential of Chitosan and Sulfated Chitosan from Cuttlebone of Sepia Aculeata Orbigny, 1848. *Asian Pac J Trop Biomed* 2012, *2*, S334–S341, doi:https://doi.org/10.1016/S2221-1691(12)60184-1.
37. Song, C.; Yu, H.; Zhang, M.; Yang, Y.; Zhang, G. Physicochemical Properties and Antioxidant Activity of Chitosan from the Blowfly Chrysomya Megacephala Larvae. *Int J Biol Macromol* 2013, *60*, 347–354, doi:10.1016/j.ijbiomac.2013.05.039.
38. Fernandes Queiroz, M.; Melo, K.; Sabry, D.; Sassaki, G.; Rocha, H. Does the Use of Chitosan Contribute to Oxalate Kidney Stone Formation? *Mar Drugs* 2014, *13*, 141–158, doi:10.3390/md13010141.